

X-ray method to study temperature-dependent stripe domains in MnAs/GaAs(001)

R. Magalhães-Paniago

Departamento de Física, Universidade Federal de Minas Gerais, CP 702, Belo Horizonte MG, 30123-970 Brazil and Laboratório Nacional de Luz Síncrotron, CP 6192, Campinas SP, 13084-971, Brazil

L. N. Coelho and B. R. A. Neves

Departamento de Física, Universidade Federal de Minas Gerais, CP 702, Belo Horizonte MG, 30123-970 Brazil

H. Westfahl

Laboratório Nacional de Luz Síncrotron, CP 6192, Campinas SP, 13084-971, Brazil

F. Iikawa

Instituto de Física "Gleb Wataghin," UNICAMP, CP 6165, 13083-970 SP, Brazil

L. Daweritz

Paul-Drude-Institut für Festkörperelektronik, Hausvogteiplatz 5-7, 10117 Berlin, Germany

C. Spezzani and M. Sacchi

Laboratoire pour l'Utilisation du Rayonnement Electromagnétique, Centre Universitaire Paris-Sud, Boîte Postale 34, 91898 Orsay, France

(Received 2 July 2004; accepted 2 November 2004; published online 27 January 2005)

MnAs films grown on GaAs (001) exhibit a progressive transition between hexagonal (ferromagnetic) and orthorhombic (paramagnetic) phases at wide temperature range instead of abrupt transition during the first-order phase transition. The coexistence of two phases is favored by the anisotropic strain arising from the constraint on the MnAs films imposed by the substrate. This phase coexistence occurs in ordered arrangement alternating periodic terrace steps. We present here a method to study the surface morphology throughout this transition by means of specular and diffuse scattering of soft x rays, tuning the photon energy at the Mn 2*p* resonance. The results show the long-range arrangement of the periodic stripe-like structure during the phase coexistence and its period remains constant, in agreement with previous results using other techniques. © 2005 American Institute of Physics. [DOI: 10.1063/1.1844599]

The integration of magnetic films in semiconductor devices represents one of the major challenges in materials science. MnAs is a very promising material for spin injection, in combination with III-V semiconductor compounds (such as GaAs).^{1,2} Around room temperature (RT), bulk MnAs undergoes a first order structural and magnetic phase transition³⁻⁵ between the low temperature α phase, hexagonal and ferromagnetic, and the high temperature β phase, orthorhombic and paramagnetic. MnAs films grown on GaAs(001)⁶⁻⁸ exhibit a phase coexistence over a temperature range that can extend between 0 and 55 °C, depending on the thickness of the film.⁹⁻¹² Several local probe techniques have been used to characterize the surface morphology and magnetic structure, such as atomic force microscopy (AFM),¹² magnetic force microscopy (MFM),¹³ and x-ray magnetic dichroism photoemission electron microscopy (XMCDPEEM).¹⁴ They highlighted the formation of periodic terraces and magnetic domains at intermediate temperatures for the phase transition. Information on the long range order of terraces is usually gained through scattering experiments. In the case of MnAs, x-ray diffraction experiments showed the coexistence of the two crystallographic phases,^{9,11} but could not address the formation of periodic domains with long range order.

In this work we have used specular and diffuse x-ray reflectivity to follow the formation and evolution with temperature of the terrace morphology throughout the α - β

phase transition. In contrast to the microscopy technique, such as atomic force microscopy, which probes small area and only near the surface, the x-ray reflectivity technique proposed here analyzes over a much larger area of the surface and deepness, providing long range order information.

A 130 nm thick MnAs was grown by molecular beam epitaxy on a GaAs(001) substrate at 250 °C in a growth condition to obtain A-type orientation,⁸ i.e., the MnAs($\bar{1}10$) plane in the α phase parallel to the GaAs (001) plane with the MnAs [0001] *c*-axis along the GaAs[$\bar{1}10$] direction.

We first used AFM to identify the terrace-like steps. Figure 1(a) depicts a room temperature AFM image of the surface topography of the MnAs film, which shows the forma-

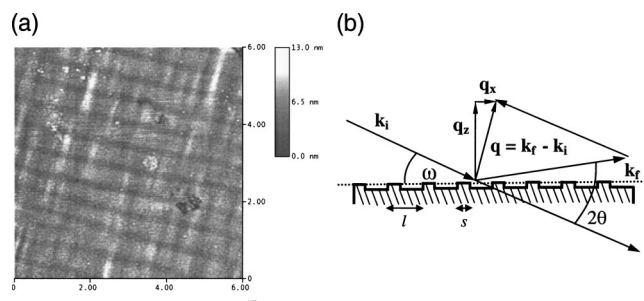


FIG. 1. (a) Atomic force microscopy image of the 130 nm thick MnAs film grown on GaAs(001); (b) scattering geometry used to examine the terrace step structure.

tion of stripe-like domains, elongated along the (0001) direction, during the coexistence of two phases and a clear alternate periodic structure between α and β phases is observed. Over the extension of the AFM image, these terrace steps appear periodic, with a modulation period of about 600 nm. The lower terraces correspond to regions where no magnetic signal is obtained with magnetic force microscopy (MFM), therefore they can be associated to the high temperature paramagnetic β phase. The higher terraces (ferromagnetic α phase) exhibit a complex magnetic structure where domains of opposite orientation seem to be intercalated.^{13,14} Several authors have already addressed the magnetic domain structure of these films using MFM techniques, and at least three different types of domain formations were observed.^{13,14} Here we will concentrate on our x-ray method to study the terrace configuration.

In order to quantitatively evaluate the surface morphology of the sample, we performed resonant x-ray scattering measurements at beamline SU-7 of the SuperACO storage ring (LURE Laboratory, Orsay). The beamline, equipped with a linear undulator source, covers the 100–1000 eV range with a resolving power of about 2000. The endstation is a two-circle ($\omega/2\theta$) reflectometer working in ultrahigh vacuum.¹⁵ As shown in Fig. 1(b), the scattering geometry was coplanar, with the incoming beam (of wave vector \mathbf{k}_i) impinging on 0.5 mm \times 0.5 mm of the MnAs film at a grazing angle ω , and the scattered photons (\mathbf{k}_f) collected at an angle 2θ with respect to the incident beam. The scattering vector $\mathbf{q}=\mathbf{k}_f-\mathbf{k}_i$ can be separated into two components, one parallel $q_x=2\pi/\lambda [\cos(2\theta-\omega)-\cos(\omega)]$ and one perpendicular $q_z=2\pi/\lambda [\sin(2\theta-\omega)+\sin(\omega)]$ to the sample surface. A structure that is periodic with a modulation period l will give rise to constructive interference in the scattering process when $q=2\pi/l$.

The reason to work at the Mn $2p$ resonance is threefold. First, the long wavelengths (~ 1.9 nm) of soft x rays are very well suited to observe large modulated structures, as is the case in our MnAs sample. The resonance increases the scattering amplitude by a factor of 10 in our case, between 600 and 640 eV, leading to an enhanced signal/noise ratio, which is very important for the analysis of weak diffuse scattering. Finally, at resonance the scattering amplitude depends on the details of the electronic structure of the scatter, leading to increased contrast between Mn ions in the α and β phases.

The horizontal terrace step structure can be studied in detail by performing rocking scans of the sample, i.e., ω scans at fixed 2θ . Over a limited range in ω around specular ($\omega=2\theta/2$), a rocking scan corresponds to a q_x scan at fixed q_z . In Fig. 2(a) we show the map of the scattered intensity that results from a series of 66 q_x scans (201 points each) performed as a function of temperature at a given q_z value (1.68 nm^{-1} , corresponding to $2\theta=30^\circ$) and photon energy (640 eV). Figure 2(b) shows the line plots of three of these scans, at temperatures corresponding to the α - β phase coexistence region. In the intermediate temperature region, we observe, besides the specular peak (zero order) at $q_x=0$, two other peaks (first order) at $q_x=\pm 0.0107 \text{ nm}^{-1}$. We ascribe them to the long range lateral order produced by the stripe domains in the phase coexistence temperature region. The associated modulation period is $l=2\pi/q_x=587 \text{ nm}$. It is worth noticing that, while the intensity of the first order peaks varies drastically as a function of temperature, their

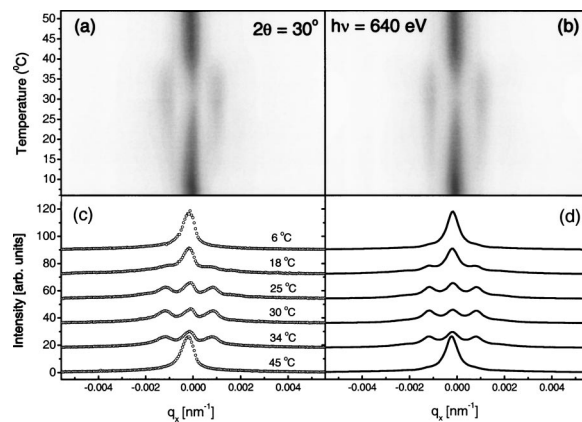


FIG. 2. (a) Two-dimensional plot of diffuse scattered intensity measured at $2\theta=30^\circ$ as a function of q_x (i.e., sample angle ω) and of temperature in the phase coexistence region and (b) corresponding fitted profiles following the model; (c) selected x-ray scans for different temperatures; (d) fitted profiles for corresponding scans on the left. Each profile was fitted separately according to Eq. (6).

position remains unaltered. This implies that the modulation period of the stripes, i.e., the sum of the widths of the two domains with different structures, remains constant. The α - β transition takes place versus temperature with the widths of the β stripe increasing at the expense of the width of the α phase, their sum remaining constant. This has been previously observed by AFM¹² and by XMCDPEEM.¹⁴

In order to reproduce the scattering profiles, a model was introduced. Following Holy *et al.*,¹⁶ the scattering intensity stemming from a lateral periodic structure is given by

$$I(q_x, q_z) = \text{const.} |C(q_x)|^2 |F(q_x, q_z)|^2. \quad (1)$$

$$F(q_x, q_z) \equiv \int_0^l e^{-iq_z h(x) - iq_x x} dx, \quad (2)$$

is the Fourier transform of the height profile function $h(x)$ of the surface, covering one terrace of each kind. In our case $h(x)$ is given by

$$h(x) = \begin{cases} 0, & \text{if } 0 < x < s \\ h_0, & \text{if } s < x < l \end{cases}, \quad (3)$$

where s is the width of the β -phase terrace and l the sum of the widths of the two terraces:

$$C(q_x) = \left\langle \sum_{m,n} \exp[-i(R_m - R_n)q_x] \right\rangle, \quad (4)$$

is the correlation function of different sets of two terraces averaged over the whole sample surface. This correlation function is proportional to a periodic sequence of δ -like functions¹⁶ centered at reciprocal lattice positions at intervals $g=2\pi/l$, resulting in

$$C(q_x) = N \left\langle g \sum_{p=-\infty}^{\infty} \delta(q_x - pg) \right\rangle, \quad (5)$$

where N is the number of periods. These δ -like functions take a Lorentzian-like line shape with full width at half-maximum σ . This finite width here represents the combination of the limited coherence length of the x-ray beam and the correlation length of the stripes. We obtain the intensity profile, which was limited to the first four reciprocal lattice points:

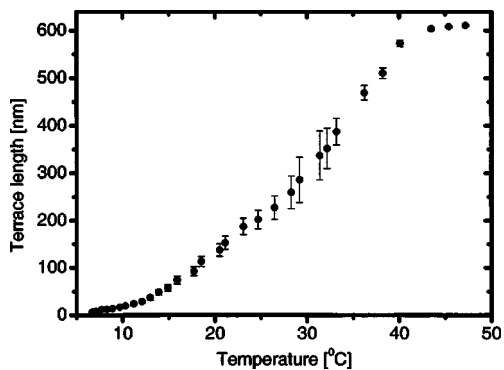


FIG. 3. Temperature dependence of the β phase terrace width. The error bars are estimated from the statistical fluctuation of the scattered intensities of the specular and first diffuse satellite peaks. The error bars are larger in the intermediate temperature region due to the lower intensity of the specular peak.

$$I(q_x, q_z) \propto |T_i T_f|^2 \left\{ \frac{s^2 + (l-s)^2 + 2 \cos(q_z h) l(l-s)}{q_x^2 + \sigma^2} + 16 \sin(hq_z/2) \sum_{p \neq 0, p=-4}^4 \frac{\sin(\pi p s/l)^2 / [p^3 (2\pi/l)^2]}{(q_x/p - 2\pi/l)^2 + \sigma^2} \right\}. \quad (6)$$

In Figs. 2(c) and 2(d) the results of calculations are compared to the corresponding experimental results of Fig. 2(a) and 2(b). The intensity profiles were fitted separately for each temperature, using s, l, σ and an overall scaling factor as fitting parameters. This model clearly reproduces extremely well the scattering data. $\sigma = (3.2 \pm 0.1) \times 10^{-4} \text{ nm}^{-1}$ remained constant throughout all measurements, which indicates that the major source of broadening comes from the limited coherence length of the x-ray beam.

In order to evaluate the relative weight of the α and β phases, one can reduce the number of fitting parameters by limiting the analysis to the ratio between the intensities of the first order peak and of the specular reflectivity. In this case the intensity ratio of these two peaks as predicted by Eq. (6) is approximately given by¹⁷

$$\frac{I(q_x = 2\pi/l)}{I(q_x = 0)} = \frac{16 \sin(hq_z/2) \sin(\pi s/l)^2 / (2\pi/l)^2}{s^2 + (l-s)^2 + 2 \cos(q_z h) l(l-s)}. \quad (7)$$

The terrace width was determined by solving numerically Eq. (7) independently from other fitting parameters. As a result, much smaller error bars for the terrace width were obtained. Figure 3 shows the temperature dependence of the β -phase terrace width.

In contrast to the surface morphologic microscopy techniques, the x-ray technique used here probes wide area and the depth of the film including also the different x-ray absorption edges to select the structures involving particular atomic elements. This will allow the determination of chemical/magnetic ordering of specific atoms belonging to the crystal lattice. The introduction of this technique will therefore be useful in special cases where microscopy techniques are not appropriate.

In summary, we demonstrate in this work that the resonant soft x-ray diffuse reflectivity method is a powerful tool to investigate microscopic structures such as the terrace-like structures of MnAs/GaAs(001) films. We observed a clear long range periodic arrangement of stripe-like microstructures alternating between α and β phases during the phase coexistence, which takes place between 10 and 45 °C. The period of the modulation structure obtained is about 600 nm, which remains constant with the temperature. The results are in good agreements with those reported in similar MnAs films using different experimental techniques.

Note added in proof. Recently satellites were observed in x-ray diffraction experiments and the average period of the domain structure was determined.¹⁸ The satellites were visible in the layer and in the substrate reflection indicating that the periodic elastic strain field due to the domain structure is penetrating into the substrate.

The authors thank M. Kästner and C. Herrmann (Paul Drude Institute) for sample growth and the personnel from LURE Laboratory for technical support. R.M-P. and H.W. thank FAPESP, CNPq, FAPEMIG, and Instituto do Milênio (Nanociências) for financial support.

- ¹M. Tanaka, *Semicond. Sci. Technol.* **17**, 327 (2002).
- ²M. Ramsteiner, R. H. Hao, A. Kawaharazuka, H. J. Zhu, M. Kästner, R. Hey, L. Däweritz, H. R. Grahn, and K. H. Ploog, *Phys. Rev. B* **66**, 081304(R) (2002).
- ³C. Guillard, *J. Phys. Radium* **12**, 223 (1951).
- ⁴B. T. M. Willis and H. P. Rooksby, *Proc. Phys. Soc., London, Sect. A* **67**, 290 (1954).
- ⁵N. Menyuk, J. A. Kafala, K. Dwinght, and J. B. Goodenough, *Phys. Rev.* **177**, 942 (1969).
- ⁶M. Tanaka, J. P. Harbison, T. Sands, T. L. Cheeks, V. G. Keramides, and G. M. Rothberg, *J. Vac. Sci. Technol. B* **12**, 1091 (1994).
- ⁷M. Tanaka, J. P. Harbison, M. C. Park, Y. S. Park, T. Shin, and G. M. Rothberg, *Appl. Phys. Lett.* **65**, 1964 (1994).
- ⁸F. Schippan, A. Trampert, L. Däweritz, and K. H. Ploog, *J. Vac. Sci. Technol. B* **17**, 1716 (1999).
- ⁹V. M. Kaganer, B. Jenichen, F. Schippan, W. Braun, L. Däweritz, and K. H. Ploog, *Phys. Rev. Lett.* **85**, 341 (2000).
- ¹⁰V. M. Kaganer, B. Jenichen, F. Schippan, W. Braun, L. Däweritz, and K. H. Ploog, *Phys. Rev. B* **66**, 045305 (2002).
- ¹¹M. Kästner, C. Herman, L. Däweritz, and K. H. Ploog, *J. Appl. Phys.* **92**, 5711 (2002).
- ¹²T. Plake, M. Ramsteiner, V. M. Kaganer, B. Jenichen, M. Kästner, L. Däweritz, and K. H. Ploog, *Appl. Phys. Lett.* **80**, 2523 (2002).
- ¹³F. Schippan, G. Behme, L. Däweritz, K. H. Ploog, B. Dennis, K.-U. Neumann, and K. R. A. Ziebeck, *J. Appl. Phys.* **88**, 2766 (2000); T. Plake, T. Hesjedal, J. Mohanty, M. Kästner, L. Däweritz, and K. H. Ploog, *Appl. Phys. Lett.* **82**, 2308 (2003); R. Engel-Herbert, J. Mohanty, A. Ney, T. Hesjedal, L. Däweritz, and K. H. Ploog, *ibid.* **84**, 1133 (2004).
- ¹⁴E. Bauer, S. Cherifi, L. Däweritz, M. Kästner, S. Heun, and A. Locatelli, *J. Vac. Sci. Technol. B* **20**, 2539 (2002).
- ¹⁵M. Sacchi, C. Spezzani, P. Torelli, A. Avila, R. Delaunay, and C. F. Hague, *Rev. Sci. Instrum.* **74**, 2791 (2003).
- ¹⁶V. Holy, T. Roch, J. Stangl, A. Daniel, G. Bauer, T. H. Metzger, Y. H. Zhu, K. Brunner, and G. Abstreiter, *Phys. Rev. B* **63**, 205318 (2001).
- ¹⁷In this procedure we have subtracted the contribution of the specular peak from the intensity of the first satellite peak, i.e., we have subtracted the nearly temperature independent component of the intensity of the first satellite. In this case, $I(q_x=2\pi/l)/I(q_x=0)$ is approximately given by the ratio of the second ($p=1$) and first terms of Eq. (6), leading to Eq. (7).
- ¹⁸B. Jenichen, V. M. Kaganer, C. Herrmann, L. Wan, L. Däweritz, and K. H. Ploog, *Z. Kristallogr.* **219**, 201 (2004).